Prediction of Turbulent Flow Behavior over a Slotted Flap

Srinath S. Heragu*
Aeronautical Development Agency, Bangalore-560017, India

The slotted flap is a wing trailing-edge device used to reduce the takeoff and landing distances of aircraft by increasing the wing maximum lift coefficient. The flow around the slotted flap, which determines the pressure distribution and effectiveness of the aerofoil system, is affected by the interaction of the wake of the main aerofoil element and the boundary layer on the flap's upper surface. This mathematical model has been developed to provide a viable calculation method, which can predict such an interaction. The system of equations has been developed in an orthogonal curvilinear coordinate system, and the principle of momentum flux balance has been effectively used in conjunction with Coles' profile for the turbulent boundary layer and a Gaussian profile for the wake. Results from this method have been compared to experimental data for three cases of flow over an aerofoil. In each case, it is shown that the displacement and momentum thicknesses, skin friction coefficient, and the merging of the wake and boundary layer predicted by this method are in good agreement with the experiment.

Nomenclature

A = constant, 5.616
B = constant, 4.8
C_f = skin friction coefficient based on the local maximum velocity; $(2U_\tau^2/U_i^2)$ in the unmerged region; $(2U_\tau^2/U_3^2)$ in the merged region
$C_{f\infty}$ = skin friction coefficient based on the freestream velocity, $2U_\tau^2$
C_p = static pressure coefficient
c = unextended chord of the aerofoil system or the chord of the aerofoil used to nondimensionalize distances
$f(x)$, $g(x)$ = polynomial functions occurring in the expression for C_p
G_1 = constant used to terminate the inner wake
G_o = constant used to terminate the outer wake
H_B = shape parameter of the boundary layer
H_{IW} = shape parameter of the inner wake
H_{ow} = shape parameter of the outer wake
$\boldsymbol{i},\boldsymbol{j},\boldsymbol{o}$ = unit vectors in the Cartesian coordinate system
k = constant, $\ell n\, 2$
L = constant, $\ell n\, 10$
L_o = nondimensional form of length scale for the outer wake
L_1 = nondimensional form of length scale for the inner wake
L_2 = length of the potential core
L_3 = thickness of the laminar sublayer that has been neglected, $= (2U_\tau/\nu)$
P = profile parameter of the boundary layer
$\boldsymbol{p},\boldsymbol{q},\boldsymbol{o}$ = unit vectors in the curvilinear coordinate system
R_{TW} = constant appearing in the eddy viscosity expression for the wake, = 40
U = nondimensional form of mean velocity in the x direction
U_e = value of U at the outer edge of the outer wake
U_i = value of U at the outer edge of the boundary layer in the unmerged case
U_o = value of U at the outer edge of the inner wake in the unmerged case
U_1 = value of U at the center of the wake
U_3 = value of U at the outer edge of the boundary layer in the merged case
U_τ = nondimensional form of friction velocity
U_∞ = freestream velocity used to nondimensionalize velocities
u = nondimensional form of turbulent velocity component in the x direction
$\boldsymbol{V}$ = resultant velocity vector
V = nondimensional form of mean velocity in the y direction
v = nondimensional form of turbulent velocity component in the y direction
X,Y,Z = Cartesian coordinates
x,y = curvilinear coordinates
$\bar{x},\bar{y}$ = distance along the aerofoil chord and perpendicular to it, divided by c
γ = intermittency factor, $= \{1 + 5.5(y/\delta)^6\}^{-1}$
δ = value of y at the outer edge of the boundary layer in the unmerged case
δ_2 = value of y at the center of the wake
δ_3 = value of y at the outer edge of the boundary layer in the merged case
δ^* = nondimensional form of displacement thickness
δ_B^* = value of δ^* for the boundary layer
δ_{IW}^* = value of δ^* for the inner wake
δ_{ow}^* = value of δ^* for the outer wake
θ = nondimensional form of momentum thickness
θ_B = value of θ for the boundary layer
θ_{IW} = value of θ for the inner wake
θ_{ow} = value of θ for the outer wake
ν = nondimensional form of kinematic viscosity
ν_t = nondimensional form of kinematic eddy viscosity
ρ = fluid density
τ = nondimensional form of shear stress

Subscripts

d = values having dimensions
T = values referring to, or derived from, total values
∞ = values in, or referred to, undisturbed stream

Received Dec. 19, 1989; revision received Nov. 21, 1990; accepted for publication Dec. 12, 1990.

*Project Manager, P.B. #1718, Vimonapura Port, Bangalore, India. Signature Analysis Group.

Introduction

FLAPS are wing trailing-edge devices that are employed to increase the maximum lift coefficient of the wing by increasing the effective camber of the aerofoil. Typical flow over a multielement aerofoil with a slotted flap is shown in Fig. 1. Many different flow models have been used to predict the lift of multielement aerofoils. Giesing[1] developed a potential flow method to simulate the flow over multiple element aerofoils. Stevens et al.[2] also used a potential flow method to predict the lift coefficient of a four-element system taking into account the attached boundary-layer development through its displacement thickness. The potential space required developed by Jacob and Steinbach[3] simulated the flow separation on the flap using a source distribution, but it could not account for the separation on the wing nor the wake shed by the wing.

The fact that the flow over the flap and, hence, the aerofoil characteristics are determined by the interaction between the wake from the main aerofoil and the boundary layer on the flap initiated experimental efforts by Foster et al.[4] and Ljungstrom.[5] However, the expensive nature of wind-tunnel testing indicated the need for numerical methods. Goradia[6] developed a confluent boundary-layer model representing the aerofoil surface by a flat plate, thus neglecting curvature effects. The flow was solved by the application of the momentum and energy integral equations to the composite region comprising the boundary layer represented by the power law and the wake by its characteristic similarity nature. In fact, this model has been incorporated by Stevens et al.[2] in their mathematical model. Irwin[7] developed a numerical method taking into account the transverse pressure gradient between the interaction of the boundary layer as represented by the power law and the wake as represented by the Gaussian profile. It was followed by Kibria,[8] who used the more reliable Coles profile to represent the flat plate boundary layer but neglected the transverse pressure gradient. Kanemoto et al.[9] undertook an experimental and theoretical effort to study flat plate boundary-layer and wake interference to understand its significance in internal flows. The log linear wall law representation was used for the boundary layer. The wake profile representation was based on a mixing length hypothesis. The velocity profile in the merged region was successfully represented by a composite profile obtained by superimposing the boundary-layer

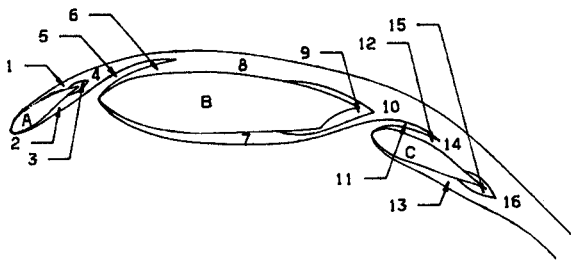

A Slat
1,2 Boundary layers on slat
3 Separated region of slat
4 Near wake region of slat
5 Potential core

B Main Aerofoil
6,7 Boundary layers on main aerofoil
8 Shear layer on main aerofoil
9 Separated region of main aerofoil
10 Near wake region of main aerofoil

C Flap
11 Potential core
12, 13 Boundary layers on flap
14 Shear layer on flap
15 Separated region of flap
16 Near wake region of flap

Fig. 1 Typical flow development on three-element aerofoil.

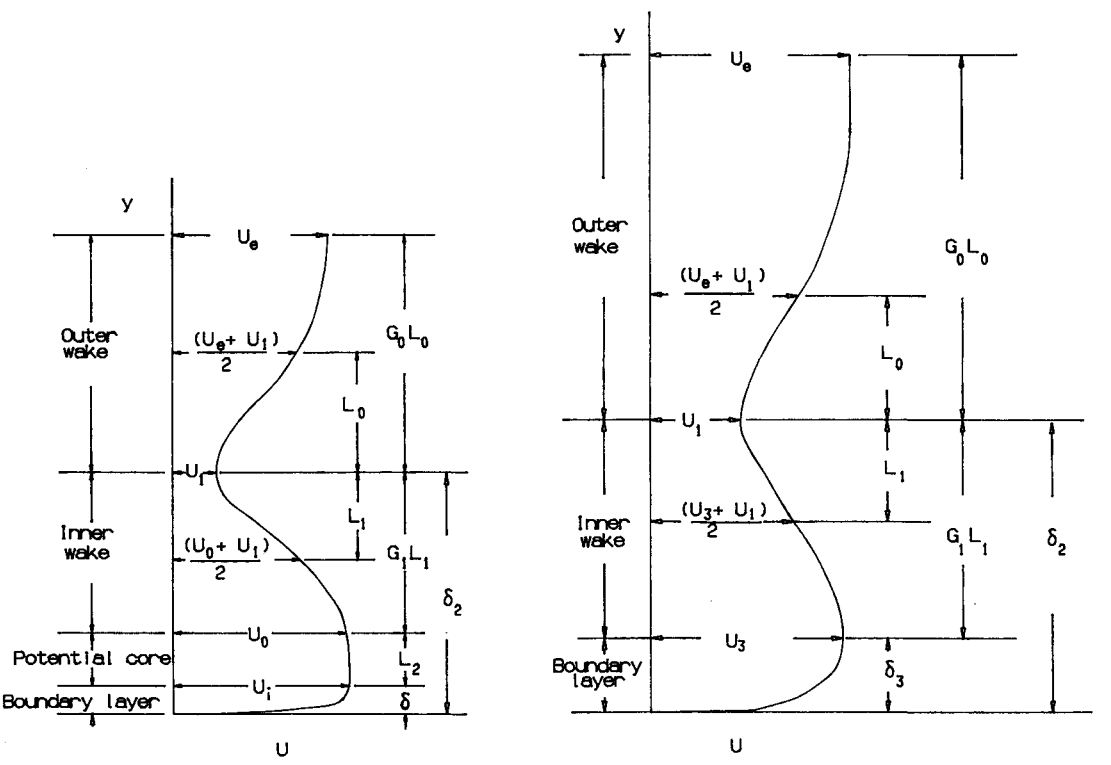

a) Unmerged region b) Merged region

Fig. 2 Typical velocity profiles on a slotted flap, with notation.

flow on the wake flow. Quite recently, Cebeci et al.[10] applied the Keller box method for the boundary-layer development, which was used for viscous correction of the potential flow modeling, but the wake was neglected.

The research presented here uses a mathematical model to predict the boundary-layer and wake interaction at subsonic speeds. This research has been inspired by the integral methods of Irwin[7] and Kibria,[8] who used the momentum integral equation as a foundation of their analyses. However, unlike these earlier researchers, the present effort examines the impact of the transverse pressure gradient on the flow over a curved surface using the exact form of the momentum integral equation.

Theory and Calculations

The development and interaction of the wake and boundary layer result in two distinct flow regimes, which are, henceforth, defined as the unmerged and merged regions. Typical velocity profiles in these regions are shown in Figs. 2. The unmerged region is that portion of the flow where the wake from the main aerofoil and the boundary layer on the flap are separated by the potential core. Farther downstream, the potential core disappears and a merged region develops where the flap boundary layer and the main aerofoil wake interact. In this analysis, the boundary layer is assumed to be fully developed and has been represented by Coles' profile given by Houghton and Boswell[11] as

$$\frac{U}{U_\tau} = \frac{A}{L}\ell_n\left(\frac{yU_\tau}{\nu}\right) + B + 2P\sin^2\left(\frac{\Pi y}{2\delta}\right) \tag{1}$$

The sub-boundary-layer region is not defined by this profile and, therefore, is not accounted for in this analysis. The Coles profile has been chosen because it satisfies the concept of equilibrium boundary layers, as suggested by Clauser,[12] for which the profile parameter P is a constant. Otherwise, for nonequilibrium boundary layers, P is a function of x. The same value for A, as suggested by Clauser,[12] has been used here.

In representing the wake, its self-preserving characteristic has been used. In fact, this self-preserving nature is assumed to occur right from the start with no mass transfer and zero shear stress at the wake center. The wake representation is similar to the one adopted by Gartshore.[13] For the outer wake

$$U = U_e - (U_e - U_1)\exp\left\{-k\left[\frac{(y-\delta_2)}{L_o}\right]^2\right\} \tag{2}$$

where L_o is the length scale, defined as the distance from the wake center to the point where the velocity is $(U_e + U_1)/2$.

For the inner wake in the unmerged region

$$U = U_o - (U_o - U_1)\exp\left\{-k\left[\frac{(y-\delta_2)}{L_1}\right]^2\right\} \tag{3}$$

where L_1 is the length scale, defined as the distance from the wake center to the point where the velocity is $(U_o + U_1)/2$. Under merged conditions, the inner wake representation is modified to the following form

$$U = U_3 - (U_3 - U_1)\exp\left\{-k\left[\frac{(y-\delta_2)}{L_1}\right]^2\right\} \tag{4}$$

Theoretically, these profiles extend to infinity. However, in this analysis, the outer wake has been terminated at $y = \delta_2 + G_oL_o$ and the inner wake at $y = \delta_2 - G_1L_1$. Following Irwin,[7] G_o has been given the value of 2.77 so that the velocity defect at the outer edge of the outer wake is 0.5%, whereas G_1 has been given a value of 2.55 so that the predicted variation of the inner wake's momentum thickness compares well with the experiment.

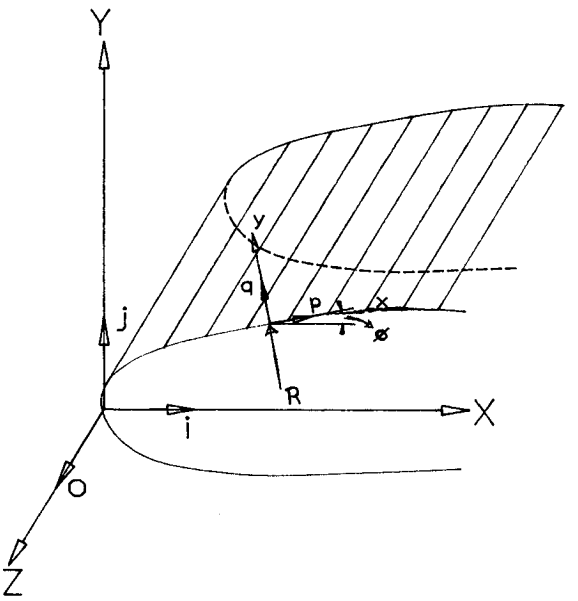

Fig. 3 Curvilinear coordinate system.

The curvilinear coordinate system shown in Fig. 3 has been used to develop the system of equations to solve the flow problem. The intermittency of the flow has been neglected everywhere except in the use of the eddy viscosity concept, whereas turbulence in the potential core and the main stream is assumed to be negligible. In this body-fitted coordinate system, x and y are the nondimensionalized distances along the flap surface and perpendicular to it. The unit vectors $\boldsymbol{p}$, $\boldsymbol{q}$, and $\boldsymbol{o}$ in this coordinate system, having the metric coefficients, $h_p = (R + y)/R$, $h_q = 1$ and $h_o = 1$, are given by

$$\boldsymbol{p} = \boldsymbol{i}\cos\phi + \boldsymbol{j}\sin\phi \tag{5a}$$

$$\boldsymbol{q} = \boldsymbol{j}\cos\phi - \boldsymbol{i}\sin\phi \tag{5b}$$

where R and ϕ are the local radius of curvature and angle of the curvilinear surface, respectively. They satisfy the three relations, $\boldsymbol{p} \times \boldsymbol{q} = \boldsymbol{o}$, $\boldsymbol{q} \times \boldsymbol{o} = \boldsymbol{p}$, and $\boldsymbol{o} \times \boldsymbol{p} = \boldsymbol{q}$, to generate the right handed system. Hence, as given by Krasnov,[14] the momentum and continuity equations in a right handed coordinate system for a compressible fluid flow with constant viscosity in the absence of mass forces can be represented vectorially as

$$\frac{\partial \boldsymbol{V}}{\partial t} + \nabla\left(\frac{V^2}{2}\right) + (\nabla \times \boldsymbol{V}) \times \boldsymbol{V} = \left(-\frac{1}{\rho}\right)\nabla C_p + \nu[\nabla(\nabla\cdot\boldsymbol{V}) - \nabla \times (\nabla \times \boldsymbol{V})] + \left(\frac{\nu}{3}\right)[\nabla(\nabla\cdot\boldsymbol{V})] \tag{6}$$

$$\partial\rho/\partial t + \nabla\cdot\rho\boldsymbol{V} = 0 \tag{7}$$

On applying the conventional order of magnitude considerations of the boundary-layer theory to the thin shear layers, the x-momentum and continuity equations for incompressible fluid flow along a surface of small curvature reduce to

$$U\frac{\partial U}{\partial x} + V\frac{\partial U}{\partial y} = -\frac{1}{2}\frac{\partial C_p}{\partial x} + \frac{\partial \tau}{\partial y} \tag{8}$$

$$\frac{\partial U}{\partial x} + \frac{\partial V}{\partial y} = 0 \tag{9}$$

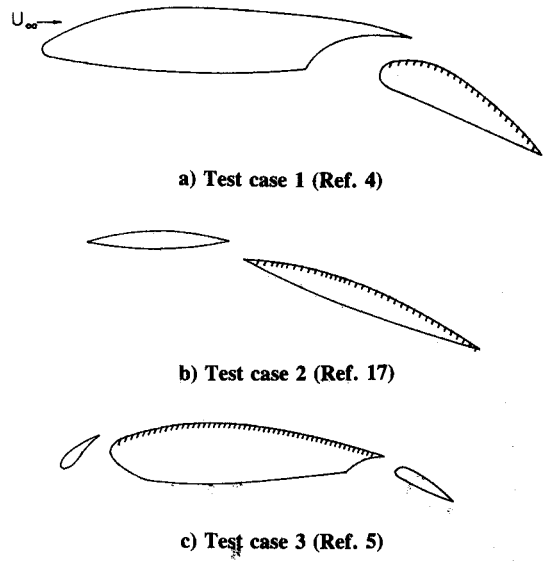

a) Test case 1 (Ref. 4)

b) Test case 2 (Ref. 17)

c) Test case 3 (Ref. 5)

Fig. 4 Aerofoil configurations used for the test cases (interaction over the hatched element has been analyzed).

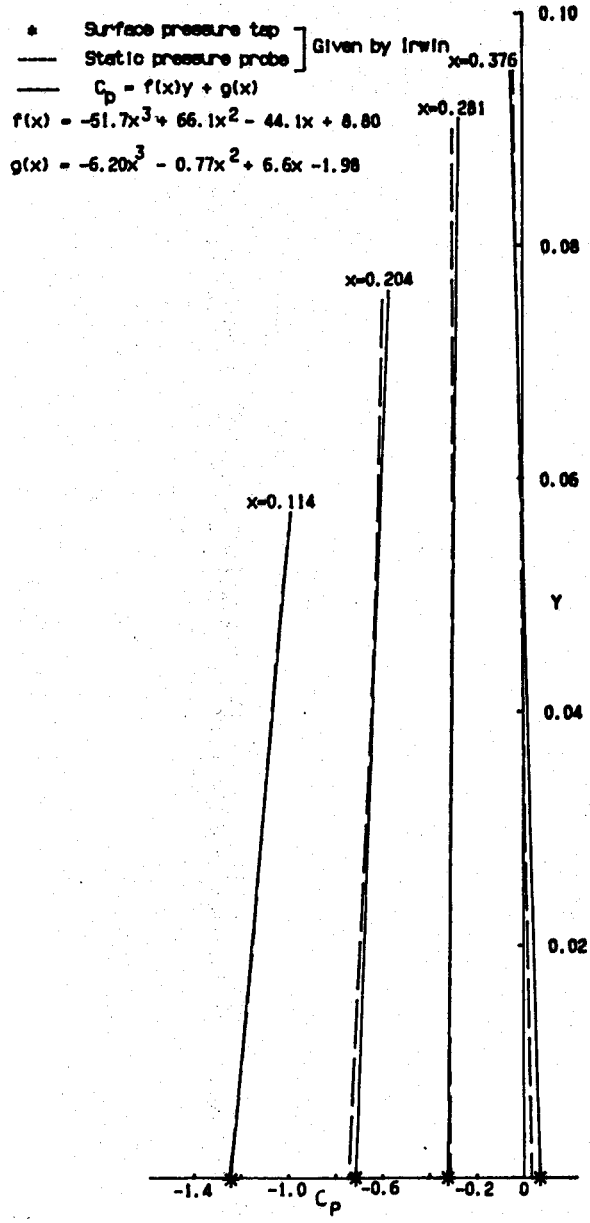

Fig. 5 Pressure field over the flap, test case 1: flap deflection 30 deg; slot gap 0.020c; angle of attack = 8 deg.

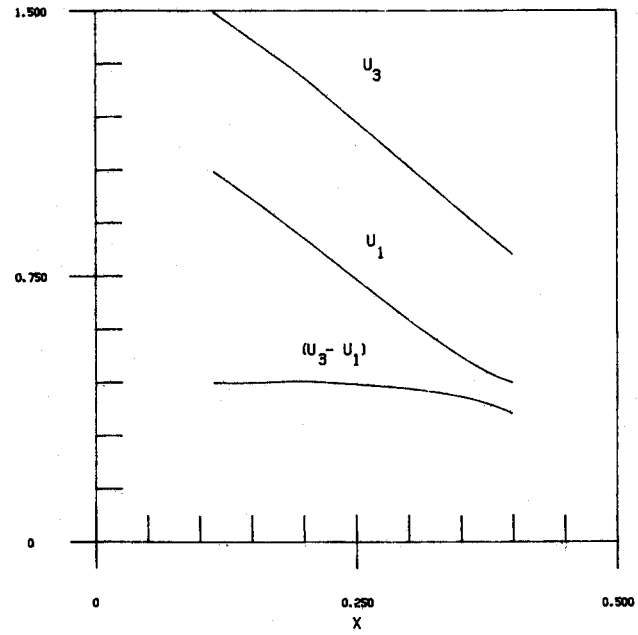

Fig. 6 Development of U_1, U_3, and $(U_3 - U_1)$ along the flap (test case 1).

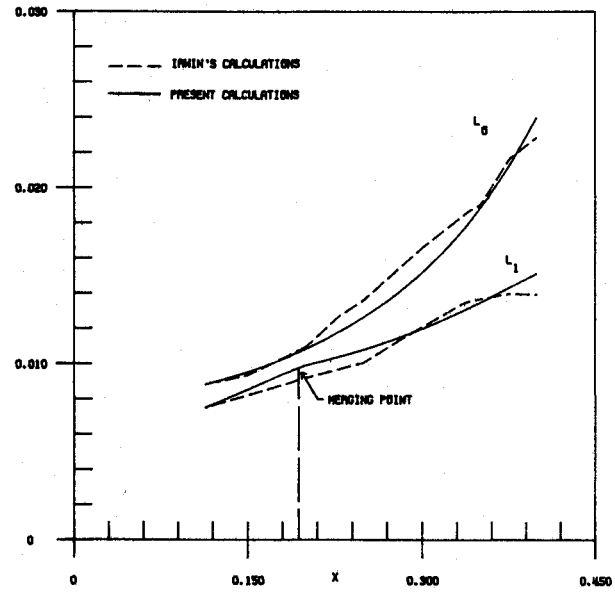

Fig. 7 Development of wake length scales L_1 and L_θ along the flap (test case 1).

These equations can be used to obtain the following momentum integral equation

$$\int_{y_1}^{y_2}\left(\frac{\partial U^2}{\partial x}\right)dy - U_{y_2}\int_0^{y_2}\left(\frac{\partial U}{\partial x}\right)dy + U_{y_1}\int_0^{y_1}\left(\frac{\partial U}{\partial x}\right)dy + \left(\frac{1}{2}\right)\int_{y_1}^{y_2}\left(\frac{\partial C_p}{\partial x}\right)dy - \tau_{y_2} + \tau_{y_1} = 0 \qquad (10)$$

for the region $y_1 \le y \le y_2$. If y_1 and y_2 are weak functions of x, the momentum integral equation may be approximated to

$$\frac{\partial}{\partial x}\int_{y_1}^{y_2} U^2 dy - U_{y_2}\frac{\partial}{\partial x}\int_0^{y_2} U\,dy + U_{y_1}\frac{\partial}{\partial x}\int_0^{y_1} U\,dy + \left(\frac{1}{2}\right)\int_{y_1}^{y_2}\left(\frac{\partial C_p}{\partial x}\right)dy - \tau_{y_2} + \tau_{y_1} = 0 \qquad (11)$$

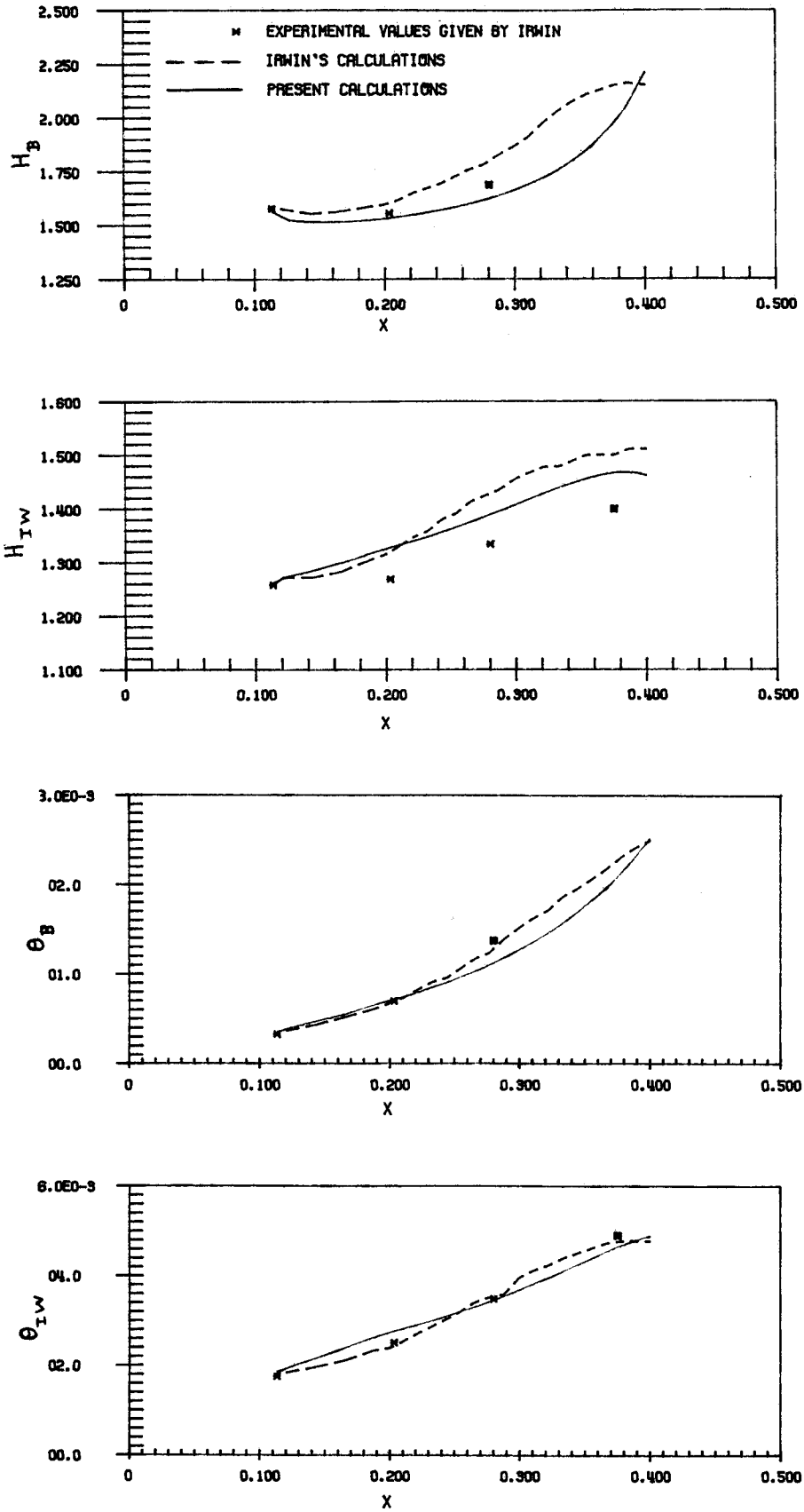

Fig. 8 Development H_B, H_{IW}, θ_B, and θ_{IW} along the flap (test case 1).

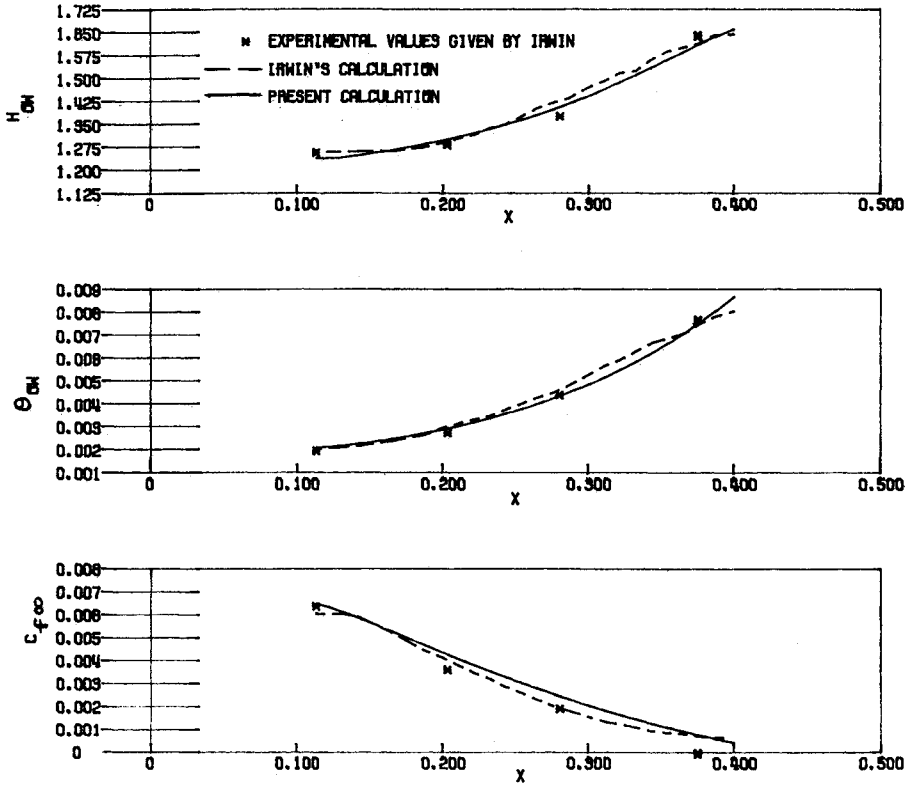

Fig. 9 Development H_{ow}, θ_{ow}, and $C_{f\infty}$ along the flap (test case 1).

as has been done by Irwin[7] and Kibria.[8] However, no such assumption has been made on the functional characteristics of y_1 and y_2 in the present analysis, and the exact form of Eq. (10) has been used. The relevant shear stresses in this equation are evaluated using the eddy viscosity concept, which is given by

$$\tau = \nu \frac{\partial U}{\partial y} - \overline{uv} = (\nu + \nu_t) \frac{\partial U}{\partial y} \approx \nu_t \frac{\partial U}{\partial y} \tag{12}$$

For the boundary-layer region, the eddy viscosity (as modified by the intermittency of the flow) is given by

$$\nu_t = (0.0168)(\delta_B^*)(U_i)(\gamma) \tag{13}$$

where the intermittency factor, as given in Ref. 15, has been used, whereas in the wake region, it is given by

$$\nu_t = (U_e - U_1) \frac{(L_o)}{R_{TW}} \tag{14}$$

Although, according to Townsend,[16] the value for R_{TW}, as determined from the equilibrium condition of eddies in a self-preserving wake flow, lies between 14 and 21, the value has been modified to account for the wake asymmetricity as suggested by Irwin.[7] The pressure field is defined as

$$C_p = f(x)y + g(x) \tag{15a}$$

where $f(x)$ and $g(x)$ are third-order polynomials in x.

The flow domain can be solved if the variables U_e, U_o, U_i, δ_2, U_1, L_o, L_1, U_τ, P, and δ along with L_2 in the unmerged region and U_3 in the merged region are known at each station. The potential flow velocities U_e, U_o, and U_i are solved from a knowledge of the pressure distribution using the relation

$$U^2 = \{1 - C_p\} \tag{15b}$$

The other variables can be solved if their corresponding derivatives $d\delta_2/dx$, dU_1/dx, dL_o/dx, dL_1/dx, dU_τ/dx, dP/dx, and $d\delta/dx$ are known. In order to solve for these derivatives, the momentum integral equation has been applied to the full thickness of the outer wake ($\delta_2 \le y \le \delta_2 + G_oL_o$), the half velocity region of the outer wake ($\delta_2 \le y \le \delta_2 + L_o$), the full thickness of the inner wake ($\delta_2 - G_1L_1$) $\le y \le \delta_2$, the full thickness of the boundary layer ($L_3 \le y \le \delta$), and the half thickness of the boundary layer ($\delta/2 \le y \le \delta$). By differentiating the relation for the velocity at the edge of the boundary layer, an additional equation is obtained. The rate of change of mass flow across the wake center, which has been assumed to be zero, and the relation $L_2 = \delta_2 - G_1L_1 - \delta$ are used to complete the system of equations noting that L_2 is zero for the merged region. Thus, a system of equations obtained in $d\delta_2/dx$, dU_1/dx, etc, is solved using the International Mathematical and Statistical Library (IMSL) routine. The details of the calculation process can be found in Ref. 15.

The calculations are started aft of the stagnation point on the flap where the flow is likely to be turbulent. The value of any variable β_{i+1} at a subsequent downstream station ($i + 1$), is obtained using the finite difference formula

$$\beta_{i+1} \approx \beta_i + \left(\frac{d\beta_i}{dx}\right) dx = \beta_i + \Delta\beta_i \tag{16}$$

where the derivatives are obtained from the solution of the system of equations. Integration and solution of the governing system of equations continues up to the trailing edge of the flap as long as $C_{f\infty}$ is positive.

As the flow develops, a situation may arise when ($U_3 - U_1$) becomes very small and the inner wake loses its identity. In this case, the entire shear layer is replaced with an equivalent boundary layer having the same total displacement and momentum thicknesses, friction velocity, and mainstream velocity. Treating the entire shear layer as one single layer, the

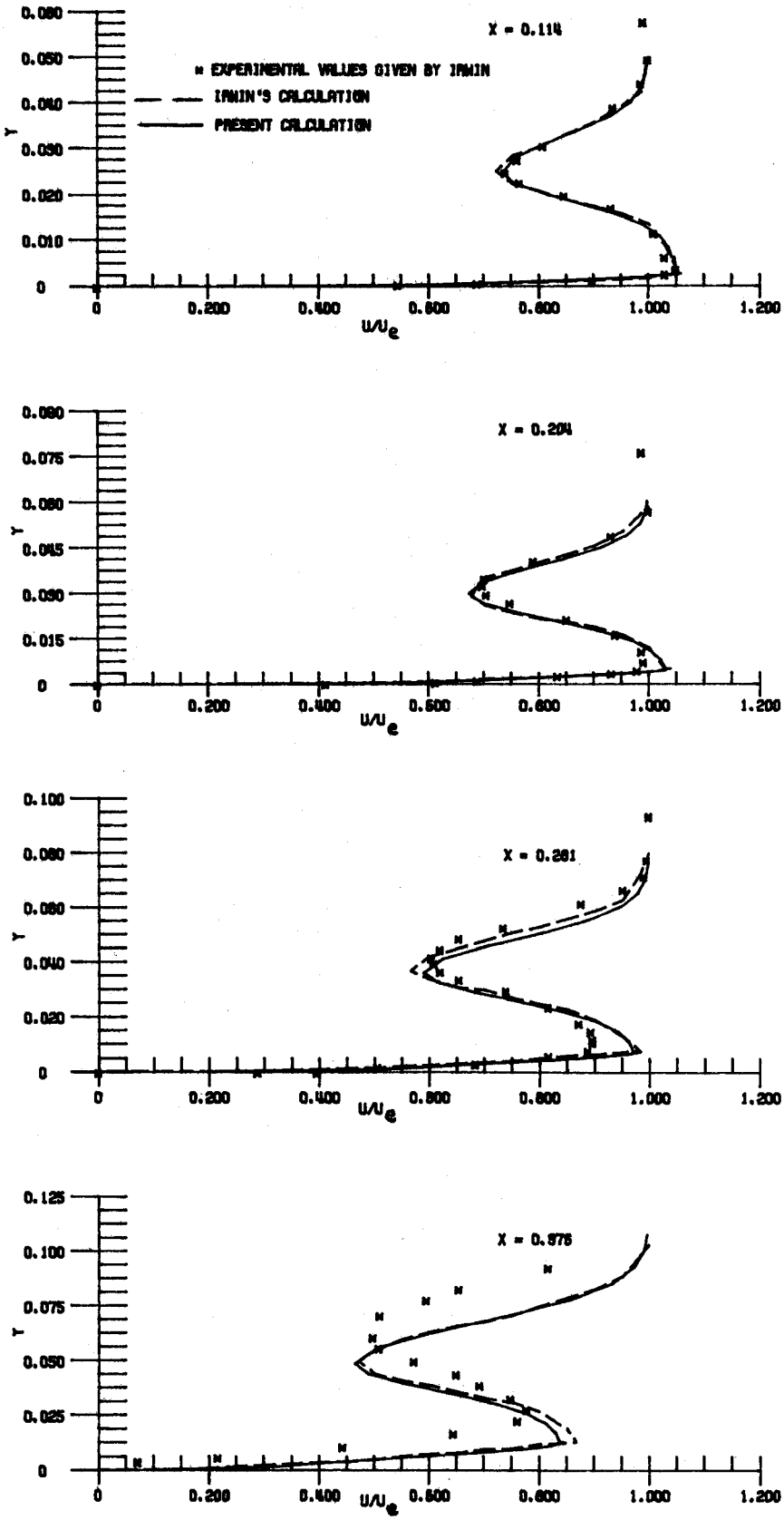

Fig. 10 Development of the velocity profiles along the flap (test case 1).

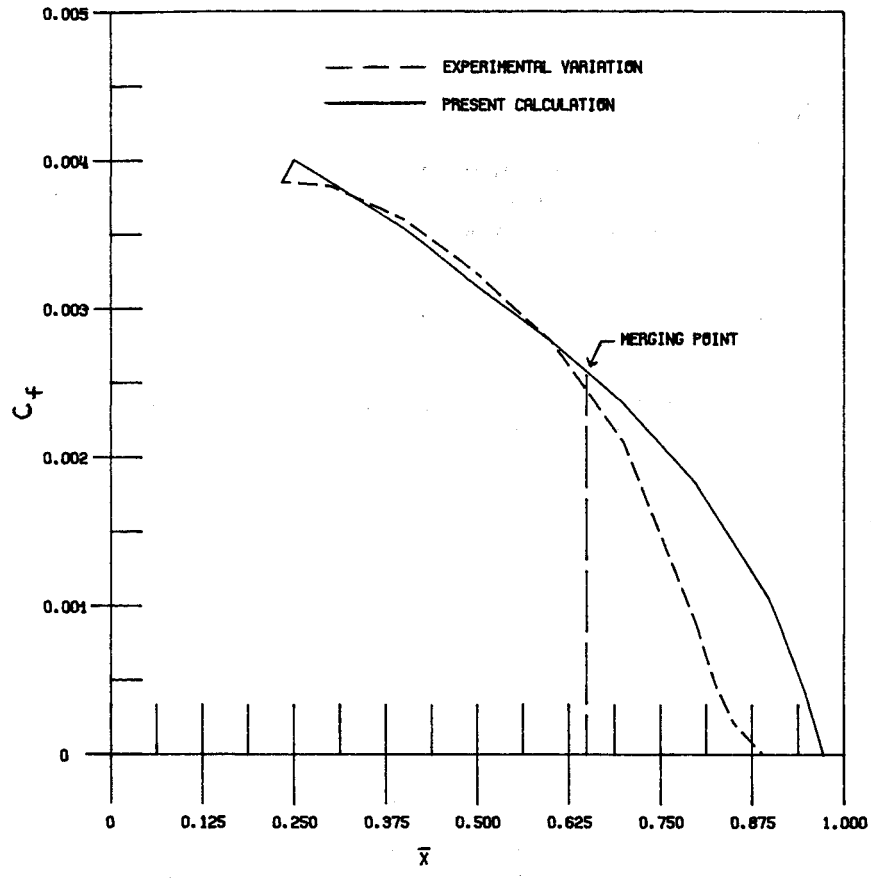

Fig. 11 Development of C_f along the aerofoil (test case 2).

total integral parameters are defined with respect to the mainstream as

$$\delta_T^* = \int_0^{\delta_2 + G_o L_o} (1 - U/U_e)\mathrm{d}y$$

$$= \int_0^{\delta_3} (1 - U/U_e)\mathrm{d}y + \int_{\delta_3}^{\delta_2} (1 - U/U_e)\mathrm{d}y + \int_{\delta_2}^{\delta_2 + G_o L_o} (1 - U/U_e)\mathrm{d}y$$

$$= (1 - U_3/U_e)\delta_3 + (U_3/U_e)\delta_B^* + (1 - U_3/U_e)G_1 L_1 + (U_3/U_e)\delta_{IW}^* + \delta_{ow}^* \quad (17)$$

$$\theta_T = \int_0^{\delta_2 + G_o L_o} (U/U_e)(1 - U/U_e)\mathrm{d}y$$

$$= \int_0^{\delta_3} (U/U_e)(1 - U/U_e)\mathrm{d}y + \int_{\delta_3}^{\delta_2} (U/U_e)(1 - U/U_e)\mathrm{d}y + \int_{\delta_2}^{\delta_2 + G_o L_o} (U/U_e)(1 - U/U_e)\mathrm{d}y$$

$$= (U_3/U_e)(1 - U_3/U_e)\delta_3 - (1 - U_3/U_e)(U_3/U_e)\delta_B^* + (U_3/U_e)^2\theta_B + (U_3/U_e)(1 - U_3/U_e)G_1 L_1 - (1 - U_3/U_e)(U_3/U_e)\delta_{IW}^* + (U_3/U_e)^2\theta_{IW} + \theta_{ow} \quad (18)$$

The integral parameters of the equivalent boundary layer by which it is replaced are given by

$$\delta_T^* = (U_\tau/U_e)\delta_T(A/L + P_T) \quad (19)$$

$$\theta_T = \delta_T^* - (U_\tau/U_e)^2\delta_T(1.5\,P_T^2 + 3.18\,AP_T/L + 2\,A^2/L^2) \quad (20)$$

Substituting for δ_T^* and θ_T from Eqs. (17) and (18) into Eqs. (19) and (20), the parameters δ_T and P_T of the equivalent boundary layer at the start of the far region are calculated, after which the rest of the far region is calculated as the equivalent boundary-layer growth.

Results and Discussions

The accuracy of this method has been verified using experimental data for the multielement aerofoils of Figs. 4. Figure 4a is the comparison to the experimental results of Foster et al.[4] for flow around a slotted flap. Figures 4b and 4c include the experimental measurements of Bario et al.[17] and Ljungstrom,[5] respectively.

Test Case 1

The aerofoil system whose geometry is shown in Fig. 4 had an unextended chord of 0.915 m. It was tested under a free-stream velocity of 61 m/s for a flap deflection of 30 deg, a slot height of 0.020c, and an angle of attack of 8 deg. Since the flap surface coordinates were not available, the flap surface has been represented by a flat plate. The experimental pressure distribution has been compared with the formulated one in Fig. 5. The curves of U_1, U_3, and $(U_3 - U_1)$ are shown in Fig. 6. In this confluence, experimental measurements indicate merging to occur ahead of $x = 0.204$, producing a strong interaction between the wake and the boundary layer, which affects their relative growth and produces an unusual variation of $(U_3 - U_1)$. The present method predicts merging

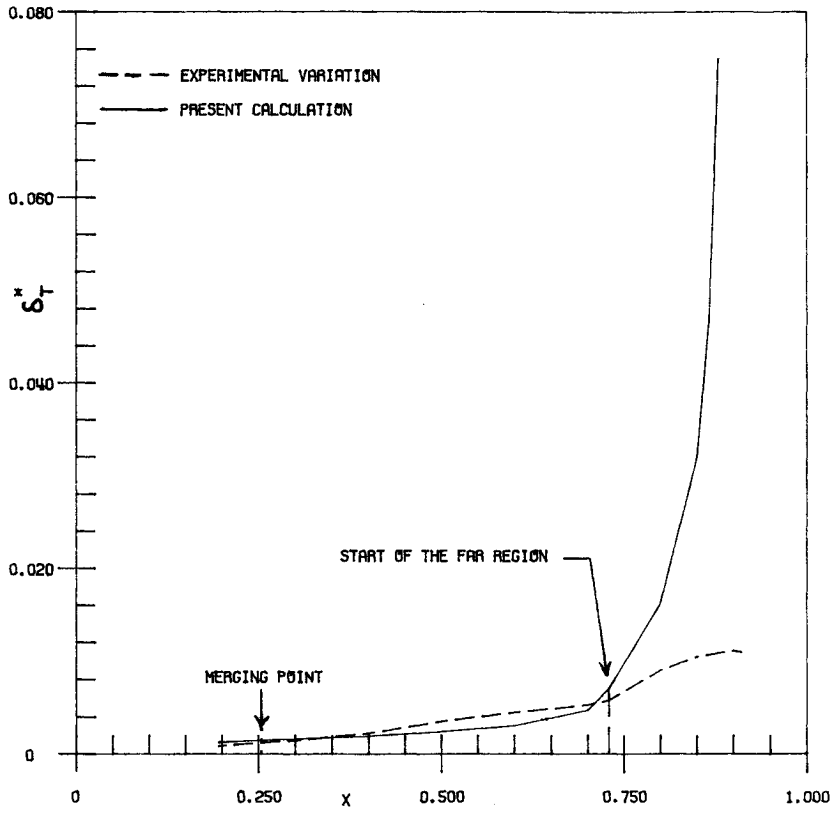

Fig. 12 Development of δ_x^* along the main aerofoil (test case 3).

to occur at about $x = 0.2$, whereas Irwin's results predict merging to occur at $x = 0.256$. The development of wake length scales, as predicted by the present method and Irwin's method, are presented in Fig. 7. The variation of L_1 predicted by this method is consistent with physical evidence, unlike Irwin's method, which does not show any increase toward the end. Theoretical results for H_B, H_{IW}, θ_B, and θ_{IW}, and that of H_{ow}, θ_{ow} and $C_{f\infty}$, are presented in Figs. 8 and 9, respectively. These show good agreement with the experimental values; whereas predicted $C_{f\infty}$ values indicate imminent separation of the flow toward the flap trailing edge. A comparison of the predicted velocity profiles with experimental data are presented in Figs. 10. The close agreement shown here supports the accuracy of the predicted integral parameters in the previous figures.

Test Case 2

A set of data for this case has been documented by Bario et al.[17] from measurements for flow over two symmetrical aerofoils in a low-speed variable pressure gradient wind tunnel. The aerofoil chord was 0.6 m and freestream velocity was 18 m/s. Based on the sectional geometry details given by Loftin,[18] a least squares fitting technique was employed to generate the following polynomial representation for the aerofoil surface.

For $0 \le \bar{x}_d \le 0.0018$:

$$\bar{y}_d^2 = 2(0.003834)\bar{x}_d - \bar{x}_d^2 \tag{21a}$$

For $0.0018 \le \bar{x}_d \le 0.24$:

$$\bar{y}_d = 2.0133\text{E-}3 + (0.7152)\bar{x}_d + (-16.0403)\bar{x}_d^2 + (214.4499)\bar{x}_d^3 + (-1477.8647)\bar{x}_d^4 + (4951.3804)\bar{x}_d^5 + (-6403.6844)\bar{x}_d^6 \tag{21b}$$

For $0.24 \le \bar{x}_d \le 0.6$:

$$\bar{y}_d = 0.1678 + (-2.4367)\bar{x}_d + (16.9103)\bar{x}_d^2 + (-58.9194)\bar{x}_d^3 + (109.5020)\bar{x}_d^4 + (-105.2700)\bar{x}_d^5 + (41.3143)\bar{x}_d^6 \tag{21c}$$

Comparisons of predicted C_f with the experiment is given in Fig. 11. Theoretical results predict merging to occur at $x = 0.65$, whereas the actual merging, as shown by the experiment, occurs at $x = 0.5$. This discrepancy is most probably attributed to the boundary layer not being fully turbulent. As a result, aft of the actual merging point, the local velocity at the boundary-layer edge is less than the velocity predicted from the pressure distribution, until the predicted merging occurs, because of the work of the shearing stresses. This will impact C_f, wherein the velocity used for normalization is the local velocity at the boundary-layer edge, causing it to be lower than prediction, so that good agreement should only be expected to occur up to the merging point.

Test Case 3

This case reviews the experimental work of Ljungstrom[5] undertaken to study the optimization of a multielement aerofoil system. As the test conditions given by Ljungstrom[5] are not detailed, the chord and the freestream velocity have been inferred as 1.1 m and 25 m/s, respectively. The experimental data have been provided as a function of the distance x along the aerofoil surface. Figure 12 shows comparisons between displacement thickness from both prediction and experiment. These results show good agreement beyond the merging point up to $x = 0.729$. Beyond this point, the inner wake loses its identity, and further calculations in this region treat the whole shear layer as an equivalent boundary layer. Unfortunately, this does not produce any further improvements in this comparison because the actual flow does not separate; whereas

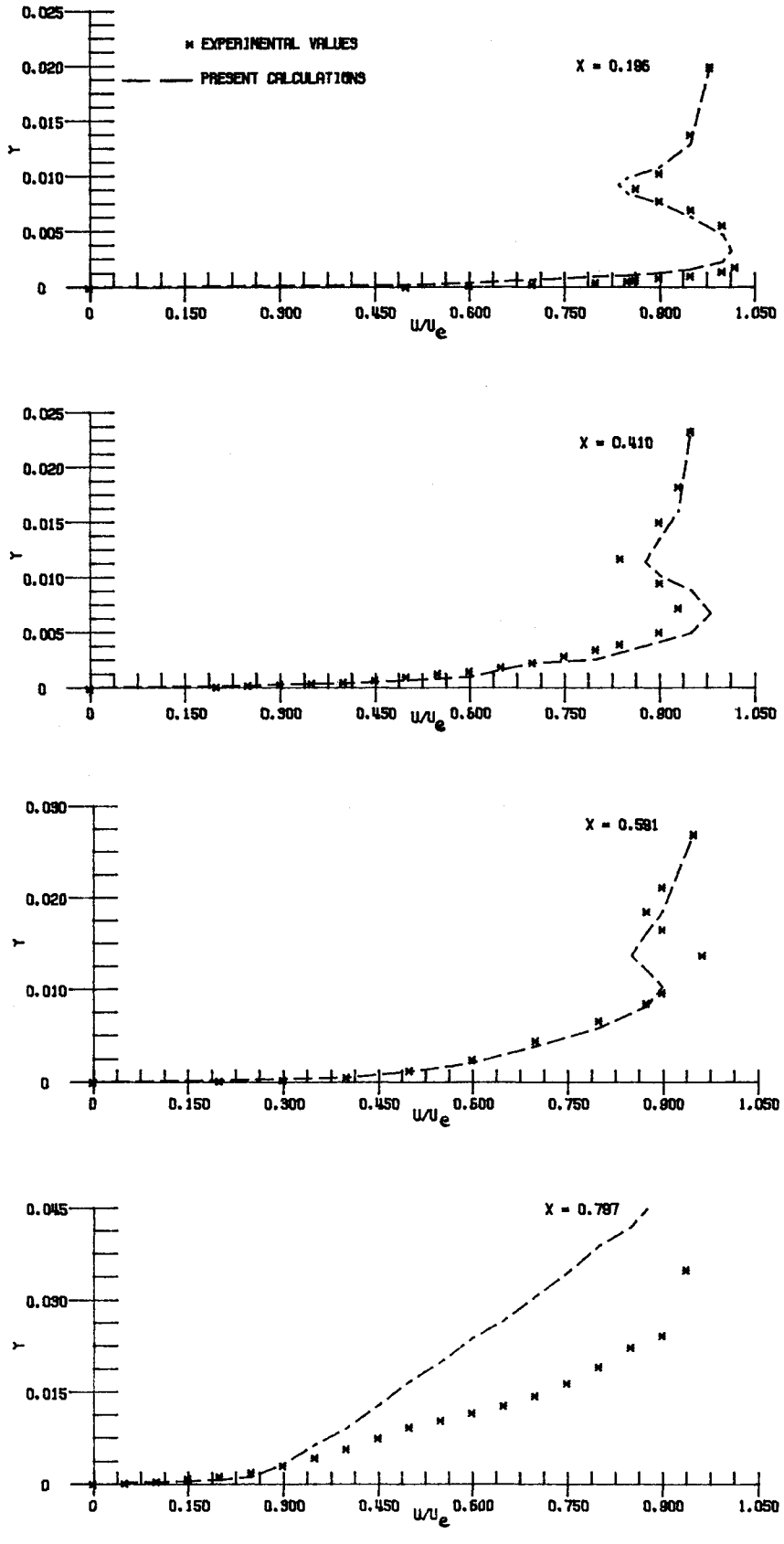

Fig. 13 Development of the velocity profiles along the main aerofoil (test case 3).

the equivalent boundary-layer calculation predicts imminent separation in this region. The loss of the inner wake's identity implies that its eddies have lost their energy by their contribution to the boundary-layer turbulence, whose intensity is more than that in an ordinary boundary-layer flow, as noted in Ref. 9. This gradual loss in the inner wake's identity is evident in Figs. 13, which show that this method does produce good comparison with the experiment for the velocity profile at all stations except at $x = 0.797$ for reasons already noted.

Conclusions

Comparison made with the experiment show good agreement with the integral parameters, the skin friction coefficient, and the location of the separation point. The prediction of these parameters has been improved by using Coles' profile for the boundary layer and incorporating the transverse pressure gradient. The prediction of the merging point and the variation of wake length scales are closer and consistent with physical reality because of the absence of assumptions in the variation of the shear layers. Further applications of this method may be in combination with potential flow models to predict more accurately the impact of viscous effects on the pressure distribution around a slotted flap aerofoil.

References

[1]Giesing, J. P., "Solutions of the Flow Field About One or More Airfoils of Arbitrary Shape in Uniform Flows by the Douglas-Neumann Method," Douglas Aircraft Co., Rept. LB 31946, Dec. 1965, 47–136.

[2]Stevens, W. A., Goradia, S. H., and Braden, J. A., "Mathematical Model for Two Dimensional Multi-Component Airfoils in Viscous Flow," NASA CR-1843, July 1971.

[3]Jacob, K., and Steinbach, D., "A Method for Prediction of Lift for Multi-Element Airfoils Systems with Separation," AGARD CP-143, Oct. 1974.

[4]Foster, D. N., Irwin, H. P. A. H., and Williams, B. R., "The Two-Dimensional Flow Around a Slotted Flap," Aeronautical Research Council Reports and Memoranda, No. 3681, 1970.

[5]Ljungstrom, B. L. G., "Experimental Study of Viscous Flow on Multi-Element Airfoils," International Council of Aeronautical Sciences, Paper 74–76, Aug. 1974.

[6]Goradia, S. H., "Confluent Boundary Layer Flow Development with Arbitrary Pressure Distribution," Ph.D. Dissertation, Georgia Institute of Technology, Atlanta, GA, Aug. 1971.

[7]Irwin, H. P. A. H., "A Calculation Method for Two Dimensional Turbulent Flow Over a Slotted Flap," Aeronautical Research Council, CP-1267, June 1972.

[8]Kibria, Md. G., "The Predicted Interaction Of a Wake With an Adjacent Turbulent Boundary Layer," M. Sc. Thesis, University of Manitoba, Winnipeg, Manitoba, Canada, 1980.

[9]Kanemoto, T., Toyokura, T., and Kurokawa, J., "Interference Between Boundary Layer Flow and Wake Flow," *Bulletin of the Japanese Society of Mechanical Engineers*, Vol. 24, No. 189, 1981, pp. 540–546.

[10]Cebeci, T., Chang, K. C., Clark, R. W., and Halsey, N. D., "Calculation of Flow over Multielement Airfoils at High Lift," *Journal of Aircraft*, Vol. 24, No. 8, 1987, pp. 546–551.

[11]Houghton, E. L., and Boswell, R. P., *Further Aerodynamics for Engineering Students*, Edward Arnold Ltd., 1969, pp. 363–375.

[12]Clauser, H. F., "Turbulent Boundary Layers in Adverse Pressure Gradients," *Journal of the Aeronautical Sciences*, Vol. 21, No. 2, 1954, pp. 91–108.

[13]Gartshore, I. S., "Two-Dimensional Turbulent Wakes," *Journal of Fluid Mechanics*, Vol. 30, Part 3, 1967, pp. 547–560.

[14]Krasnov, N. F., *Aerodynamics*, Amerind Publishing Co., Pvt, Ltd., 1978, pp. 59–99.

[15]Heragu, S. S., "The Predicted Behaviour of Two Dimensional Flow Over a Slotted Flap," M. Sc. Thesis, University of Manitoba, Winnipeg, Manitoba, Canada, 1984.

[16]Townsend, A. A., *The Structure of Turbulent Shear Flow*, Cambridge University Press, 1956, pp. 126–130.

[17]Bario, F., Charnay, G., and Papailiou, K. D., "An Experiment Concerning the Confluence of a Wake and a Boundary Layer," Transactions of the American Society of Mechanical Engineers, *Journal of Fluids Engineering*, Vol. 104, No. 1, 1982, pp. 18–24.

[18]Loftin, L. K., Jr., "Theoretical And Experimental Data for a Number of NAC 6A-Series Airfoil Sections," NACA Rept. 903, 1948.